

## Waves in Random and Complex Media

ISSN: (Print) (Online) Journal homepage: <https://www.tandfonline.com/loi/twrm20>

# Impact of geometric shape of cavity on heat exchange using Cu-Al<sub>2</sub>O<sub>3</sub>-H<sub>2</sub>O hybrid nanofluid

Kamel Chadi, Mouna Maache Battira, Momen S. M. Saleh, Nourredine Belghar, Mohammed Lachi & Ali J. Chamkha

To cite this article: Kamel Chadi, Mouna Maache Battira, Momen S. M. Saleh, Nourredine Belghar, Mohammed Lachi & Ali J. Chamkha (2022): Impact of geometric shape of cavity on heat exchange using Cu-Al<sub>2</sub>O<sub>3</sub>-H<sub>2</sub>O hybrid nanofluid, *Waves in Random and Complex Media*, DOI: 10.1080/17455030.2022.2134606

To link to this article: <https://doi.org/10.1080/17455030.2022.2134606>



Published online: 19 Oct 2022.



Submit your article to this journal [↗](#)



Article views: 78



View related articles [↗](#)



View Crossmark data [↗](#)



## Impact of geometric shape of cavity on heat exchange using Cu-Al<sub>2</sub>O<sub>3</sub>-H<sub>2</sub>O hybrid nanofluid

Kamel Chadi<sup>a</sup>, Mouna Maache Battira<sup>b</sup>, Momen S. M. Saleh<sup>c</sup>, Nourredine Belghar<sup>a</sup>, Mohammed Lachi<sup>d</sup> and Ali J. Chamkha<sup>e</sup>

<sup>a</sup>Laboratory of Materials and Energy Engineering, Mohamed Khider University, Biskra, Algeria; <sup>b</sup>Department of Mechanical Engineering, Science and Technology Faculty, Abbes Laghrour University, Khenchela, Algeria; <sup>c</sup>Laboratory of Industrial Technologies, Ibn Khaldoun University, Tiaret, Algeria; <sup>d</sup>MATIM, University of Reims Champagne Ardennes, Reims, France; <sup>e</sup>Faculty of Engineering, Kuwait College of Science and Technology, Doha, Kuwait

### ABSTRACT

In the present work, the impact of cavity geometric shape on heat exchange is numerically studied. The Cu-Al<sub>2</sub>O<sub>3</sub> water hybrid nanofluid with a solid volume fraction of 0,03 is considered in this simulation. The bottom wall of the cavity is brought to a constant hot temperature. The two vertical side walls are cooled, and the upper wall of the cavity is adiabatic.

In these conditions, four cases are studied. The first one is a rectangular cavity filled with the hybrid nanofluid, while in each case of the other three, the shape of one cavity wall is changed. The numerical results are developed for Rayleigh numbers varying from 10<sup>3</sup> to 10<sup>5</sup> and for a laminar and stationary flow regime. The governing equations are solved numerically using the finite volume method (FVM).

The results indicate that the cavity shape significantly affects the improvement of heat exchange. We found that the third case gives the best heat exchange compared to the other cases, and the increase in the value of the Rayleigh number contributes to an enhancement in heat exchange, especially in the third case. It also participates in a decrease in the temperature inside the cavity.

### ARTICLE HISTORY

Received 1 April 2022  
Accepted 4 October 2022

### KEYWORDS

Hybrid nanofluid; Rayleigh number; numerical simulation; cavity; heat exchange

## Nomenclature

- $C_p$ : specific heat of the fluid, J.kg<sup>-1</sup>.K<sup>-1</sup>  
 $g$ : acceleration of gravity, m.s<sup>-2</sup>  
 $Gr$ : Grashof number  
 $H$ : cavity height, m  
 $k$ : thermal conductivity, W.m<sup>-1</sup>.K<sup>-1</sup>  
 $L$ : cavity length, m  
 $Nu_L$ : local Nusselt number  
 $P$ : pressure, Pa  
 $Pr$ : Prandtl number

**CONTACT** Kamel Chadi  [chadikamel\\_dz@yahoo.fr](mailto:chadikamel_dz@yahoo.fr)

- $T$ : temperature, K  
 $T_c$ : temperature of bottom wall of cavity, K  
 $u, v$ : velocity components,  $\text{m}\cdot\text{s}^{-1}$   
 $U, V$ : dimensionless velocity components form  
 $x, y$ : cartesian coordinates, m  
 $X, Y$ : dimensionless cartesian coordinates

## Indices

- $f$ : base fluid (water)  
 $hnf$ : hybrid nanofluid  
 $nf_1$ : Cu-water nanofluid  
 $nf_2$ :  $\text{Al}_2\text{O}_3$ -water nanofluid

## Greek symbols

- $\alpha$ : thermal diffusivity,  $\text{m}^2\cdot\text{s}^{-1}$   
 $\beta$ : thermal expansion coefficient,  $\text{K}^{-1}$   
 $\theta$ : dimensionless temperature  
 $\mu$ : dynamic viscosity of coolant,  $\text{kg}\cdot\text{m}^{-1}\cdot\text{s}^{-1}$   
 $\rho$ : coolant density,  $\text{kg}\cdot\text{m}^{-3}$   
 $\varphi$ : nanoparticle volume fraction

## 1. Introduction

Thermal transfer in cavities is a scalable topic that can be applied in several fields, such as cooling electronic components, thermal and nuclear installations, building industry, etc. Researchers in this field have presented several solutions to improve heat exchange inside the cavities. Among which are the insertion of porous media, the addition of barriers inside the cavity, the changing of the cavity shape, the use of hybrid fluids, and the use of the magnetic field (MF). Mahmoodi et al. [1] presented a numerical study of the fluid flow by free convection and the heat exchange of Cu- $\text{H}_2\text{O}$  nanofluid within a square cavity whose center contains an adiabatic square body. They discretized the governing equations using the finite volume method (FVM) and used the SIMPLER algorithm for velocity-pressure coupling. They also shed light on the effect of the copper nanoparticle volume fraction, the Rayleigh number ( $Ra$ ), and the size of the adiabatic square body on the thermal fields and the liquid flow. Their results indicate that the mean Nusselt number ( $Nu$ ) rises with the rising volume concentration of nanoparticles at all  $Ra$  numbers except for  $Ra = 10^4$ . Moreover, with a lower  $Ra$  number ( $10^3$  and  $10^4$ ), the thermal exchange rate reduces with the growth of the adiabatic square body dimensions, where as at a high  $Ra$  number ( $10^5$  and  $10^6$ ), it enhances.

Aminossadati et al. [2] studied the magne to hydrodynamics of Cu- $\text{H}_2\text{O}$  nanofluid within a triangular enclosure. The study shows that the increase in  $Ra$  number conducts to an intensification of convective currents. In addition, increasing the Hartmann number ( $Ha$ ) reduces heat transfer and removes recirculation cells. Additionally, the study out comes reveal that adding nanoparticles increases the  $Nu$  at low  $Ra$  number values.

Mehmood et al. [3] utilized the KKL model for investigating the mixed convection of Al-H<sub>2</sub>O nanofluid in a square porous enclosure. They examined the influence of the non-linear model of radiation and the inclined MF effect. The study results showed that the maximum stream function rises when the porosity intensifies. In addition, a significant reduction in the mean  $Nu$  is explored with an increasing MF inclined angle.

Rahmati et al. [4] simulated the free convection of water-TiO<sub>2</sub> nanofluid around a hot obstacle in a square enclosure using the Lattice Boltzmann method. The impact of  $Ra$  number, obstacle dimensions, the volume fraction of the nanofluid, and enclosure sizes on  $Nu$  and thermal transfer rate around the hot obstacle in the enclosure are analyzed. The simulation findings indicated that with increasing the  $Ra$  number and volume concentration, the average  $Nu$  augments. Further, the average  $Nu$  increases with increasing the enclosure length and decreases with increasing enclosure width. They also found that the average  $Nu$  in Wang's model is lower than  $Nu$  in Brinkman's model.

Mohebbi et al. [5] carried out a two-dimensional numerical investigation of the impact of MF on forced convection of Ag/MgO nanofluid and thermal exchange in a conduit with active coolers and heaters. For this purpose, a FORTRAN code was developed, and the impacts of thermal arrangement (case 2, 3, and 1),  $Ha$  number (0 to 60), Reynolds number (50 to 100), and volume concentration of nanoparticles  $\varphi$  (0 to 0.02) on flow configuration and on heat exchange properties was examined. Results indicated that the most significant value of the local  $Nu$  occurs at the junction of the cooler and the heater. Their numbers also indicate that the thermal exchange rate increases with increasing  $\varphi$  or decreasing  $Ha$  number, and the thermal exchange rate in case 1 is more significant than in the others.

Ghalambaz et al. [6] studied convection stream of Ag-MgO/H<sub>2</sub>O hybrid nanofluid in a square enclosure. They calculated the thermo-physical properties of the nanofluid by using experimental data. They studied the impact of dimensionless parameters such as  $Ra$  number, the volume concentration of nanoparticles, and the thermal conductivity ratio on temperature distribution and the variation of the average  $Nu$  and the local  $Nu$ . Their results showed that the rate of heat transfer increases by adding hybrid nanoparticles for low  $Ra$  number. For high  $Ra$  number, they found that the local  $Nu$  at the surface of the conjugate wall reduces by displacing from the bottom of the enclosure toward the top.

Rizwan et al. [7] presented a two-dimensional numerical study of free convection in a trapezoidal enclosure filled with copper oxide water nanofluid with an internal heater trapezium. In this study, they relied on the Finite Element Method (FEM) to achieve the appropriate outcomes in stream function and isothermal inside the limited field of the enclosure. The study was performed for the  $Ra$  number between  $10^4$  and  $10^{5.7}$ . Their results show that the flow and the heat field rise with increasing  $Ra$  number. They also found that the liquid velocity decreased with the enhancement in the NPS volume concentration.

Chakkingal et al. [8] investigated the natural convection in an enclosure heated from below and cooled from its upper wall, entirely and partially filled with adiabatic spheres arranged in a cubic packing. They studied the impact of packing size and the position of porous media. In this study, they considered  $Ra = 1.16 \times 10^5$ ,  $1.16 \times 10^6$  and  $2.31 \times 10^7$ . Among the most important results is that the cavity's heat transfer decreases when the porous medium is close to the isothermal walls. It was remarked that when the thermal boundary layer thickness is greater than the pore space, the location and number of packing layers modify the heat exchange rate.

Armaghani et al. [9] presented numerical research on the impact of source/sink setting and size on MHD mixed convection in  $\text{Al}_2\text{O}_3\text{-Cu/Water}$  hybrid nanofluid filling an L-shaped enclosure. Two uniform thermal sources are placed in the lower corners of the enclosure. The impact of several thermo-physical parameters such as MF,  $Ha$ , sink/source location and power and length ratio, the angle, and the volume fraction of copper (Cu) and alumina ( $\text{Al}_2\text{O}_3$ ) and their combination nanoparticles seeded in water are studied. Among the most important results, the MF angle which leads to the best heat exchange efficacy is 180. Also, the concentration of nanoparticles increases thermal performance, and the most significant thermal efficacy corresponds to the case ( $L_1 = 0.8, L_2 = 0.2$ ).

Among the most important recent research work, we find Hassan et al. [10] did a microscopic study of natural convection due to  $\text{Fe}_3\text{O}_4\text{-MWCNT/H}_2\text{O}$  hybrid nanofluid using the Lattice Boltzmann method. They filled the test fluid into a differentially heated rectangular enclosure. This study demonstrates the impacts of  $Ra$  number from  $10^3$  to  $10^5$ , aspect ratio from 0.5 to 2.0, and nanocomposite concentration volume on heat and liquid flow properties and entropy generation. They observed that the average  $Nu$  rises with an increase in the  $Ra$  number, while it decreases with an increase in the aspect ratio. They also observed that the  $Ra$  number increases with the number of dimensionless entropy generation increases. They also found that increasing nanoparticles loading fraction helps increase the entropy generation number. They also concluded that the better heat transfer for the enclosure of 0.5 aspect ratio.

Chamkha et al. [11] studied numerically and using the finite element method (Galerkin method), the heat transfer by mixed convection in the enclosure with a wavy-walled lid containing a conductive square solid. Using a  $\text{Cu-Al}_2\text{O}_3\text{-H}_2\text{O}$  hybrid nanofluid, one of the primary objectives of this study is to examine the effect of the two-phase hybrid nanofluid approach on conduction and convection properties, including the consequences of Richardson number difference, nanoparticle concentration volume, number of oscillations, the solid obstacle position and dimensionless length, where they found that imposing specific undulations on the walls of vertical active helps in enhancing the heat transfer and distributions of the nanoparticles within the cavity.

Geridonmez et al. [12] conducted a numerical study on the natural heat flow of  $\text{Ag-MgO-H}_2\text{O}$  hybrid nanofluid in a trapezoidal formed enclosure under the influence of partial magnetic fields. This research also relied on the Brinkmann model of dynamic viscosity and Xue's thermal conductivity model. They concluded in the last that the large area of influence area of the partial magnetic field leads to the inhibition of liquid flow and thermal transfer.

On the other hand, Aly et al. [13] studied the effects of magnetic field on mixed convective flux inside a corrugated cavity filled with porous media and hybrid nanofluids. They considered the plane walls to be adiabatic and the vertical corrugated walls of the cavity to have a temperature of  $T_c$ . The bottom wall of the cavity is heated, and the top left walls have lid velocities. They also used the finite volume method by SIMPLE technique to solve dimensionless control equations. Among the essential results they reached is that the position and length of the heater are efficient in improving the movements of nanofluid and the thermal performance within an undulating cavity. Increasing the thermal radiation coefficient and the heat absorption/generation coefficient improves the solid phase isotherms.

Sudarsana and Sreedevi [14] numerically examined fluid entropy generation, flow and heat transfer within the closed chamber by magnetic field attraction using a hybrid liquid

nanofluid and using finite element method; their results which are schematic diagrams, indicate that the heat gradient of single-walled carbon nanotubes is higher than that of silver nanoparticles. The heat transfer rate increases from 6.2% to 15.6% in the case of single-walled carbon nanotubes with a volume fraction of 0.05 suspended in the base liquid, while the thermal transfer rate rises from 6.2% to 10.4% in the case of volume fraction silver nanoparticles 0.05 suspended in the base liquid.

Another recent study [15] examined the impact of hybrid nanofluid flow under the influence of a magnetic field in a compact tube applied in a fixed magnetic field. They also used a hydrothermal behavior of 1.0% vol.  $\text{Fe}_3\text{O}_4$ /water, 1.0% vol. Cu/water as mono-nanofluid and 0.5% vol.  $\text{Fe}_3\text{O}_4$ -0.5% vol. They also examined Cu/water as a hybrid nanofluid in the rammed tube under the condition of the laminar flow regime  $Re$  number = [1131-2102] and the constant heat flux.

Among the essential results they obtained is that the magnetic field affects enhancing the Nusselt number ( $Nu$ ) and the friction factor and that the flow of hybrid nanofluids in the dredged tube, the magnetic field with the magnitude of 0.3 Tesla leads to an increase in the  $Nu$  and the friction factor.

The study Haokun and Yit Fat [16] conducted dealt with the heat transfer and the flow of hybrid nanofluids in a curved porous channel. This study included the various transfer processes (i.e., momentum, mass, and energy). They also validated the model's performance to check the flow and thermal transfer of the  $\text{Al}_2\text{O}_3$ -Cu- $\text{H}_2\text{O}$  hybrid nanofluid. Their results showed that the thermal transfer increases with a raised volume fraction of nanoparticles, higher, more significant porosity, and Reynolds number ( $Re$ ).

Nazar et al. [17] analyzed the unstable mixed convection of the  $\text{Al}_2\text{O}_3$ -Cu/water hybrid nanofluid flow past a vertical plate close to the stagnation point. They used the bvp4c technique to solve the resulting differential equations. In this study, they studied the impacts of several relevant physical factors. Their results showed that the rate of heat transfer decreases when the concentration volume of the nanoparticles rises, and they also found that the parameter of the slip is proven to raise the skin friction coefficient while the local  $Nu$  decreases in the buoyancy opposing flow.

This work aims to study the natural convection in the various geometric shapes of the cavities to obtain the appropriate cavity shape, which contributes to increasing the heat exchange of the hybrid nanofluid.

## 2. Thermo-physical properties of hybrid nanofluid

The effective thermal conductivity of the hybrid nanofluid ( $h_{nf}$ ) is given by [18]:

$$k_{h_{nf}} = \left[ \frac{(\varphi_{nf2}k_{nf2} + \varphi_{nf1}k_{nf1})}{\varphi_{h_{nf}}} + 2k_f + 2(\varphi_{nf2}k_{nf2} + \varphi_{nf1}k_{nf1}) - 2\varphi_{h_{nf}}k_f \right] \times \left[ \frac{(\varphi_{nf2}k_{nf2} + \varphi_{nf1}k_{nf1})}{\varphi_{h_{nf}}} + 2k_f - (\varphi_{nf2}k_{nf2} + \varphi_{nf1}k_{nf1}) + \varphi_{h_{nf}}k_f \right]^{-1} \quad (1)$$

Where:  $\varphi_{h_{nf}} = \varphi_{nf1} + \varphi_{nf2}$

The density of the hybrid nanofluid ( $h_{nf}$ ) is given by [18]:

$$\rho_{h_{nf}} = \varphi_{nf2}\rho_{nf2} + \varphi_{nf1}\rho_{nf1} + (1 - \varphi_{h_{nf}})\rho_f \quad (2)$$

**Table 1.** Thermophysical properties of the water and nanoparticles.

	$\rho$ [kg/m <sup>3</sup> ]	$C_p$ [J/(kg.K)]	$K$ [W/(m.K)]	$\mu$ [kg/(m.s)]	$\beta$ [1/K]
Water	997.1	4179	0,613	0.001003	$21 \times 10^{-5}$
Cu nanoparticles	8933	385	401	–	$1.67 \times 10^{-5}$
Al <sub>2</sub> O <sub>3</sub> nanoparticles	3970	765	40	–	$0.85 \times 10^{-5}$

The dynamic viscosity is expressed by [18]:

$$\mu_{hnf} = [1 - (\varphi_{nf1} + \varphi_{nf2})]^{-2.5} \mu_f \quad (3)$$

The heat capacitance of the hybrid nanofluid (*hnf*) is expressed by [18]:

$$(\rho C_p)_{hnf} = \varphi_{nf2}(\rho C_p)_{nf2} + \varphi_{nf1}(\rho C_p)_{nf1} + (1 - \varphi_{hnf})(\rho C_p)_f \quad (4)$$

The thermal expansion coefficient of the hybrid nanofluid (*hnf*) is expressed as given by [18]:

$$(\rho\beta)_{hnf} = \varphi_{nf2}(\rho\beta)_{nf2} + \varphi_{nf1}(\rho\beta)_{nf1} + (1 - \varphi_{hnf})(\rho\beta)_f \quad (5)$$

The thermo-physical properties of water and nanoparticles are grouped in Table 1 [19]

### 3. Geometrical system

The field of study is a two-dimensional rectangular enclosure where the dimensions are length  $L$  and width  $H$ . The enclosure is filled with Cu-Al<sub>2</sub>O<sub>3</sub> /water hybrid nanofluid. Four cases with identical boundary conditions are presented.

The first case is a rectangular enclosure whose bottom wall is fixed at a constant hot temperature ( $T_h$ ), the two vertical walls of the enclosure are maintained isothermally at a temperature ( $T_c$ ) lower than the temperature of the bottom wall, and the upper wall of the cavity is considered as adiabatic.

The second case: The shape of the cavity's right vertical wall in the first case is changed (Figure 1b).

The third case: The shape of the cavity's right and left vertical walls of the first case is changed (Figure 1c)

Fourth case: The shape of the cavity's upper horizontal wall in the first case is changed (Figure 1d).

The corresponding boundary conditions for the four cases are given by:

- All walls :  $U = 0, V = 0$
- Top wall:  $0 \leq X \leq 1; Y = 1; (\partial\theta/\partial Y) = 0$
- Right and left sidewalls: Right wall  $X = 1; 0 \leq Y \leq 1; \theta = 0$
- left wall  $X = 0; 0 \leq Y \leq 1; \theta = 0$
- Bottom wall:  $0 \leq X \leq 1; Y = 0; \theta = 1;$
- **Simplifying Hypothesis:**
  - Newtonian and incompressible fluid.
  - Two-dimensional flow in cartesian coordinates.
  - Laminar and permanent flow regime.
  - Absence of internal heat source, mass source or chemical reaction.

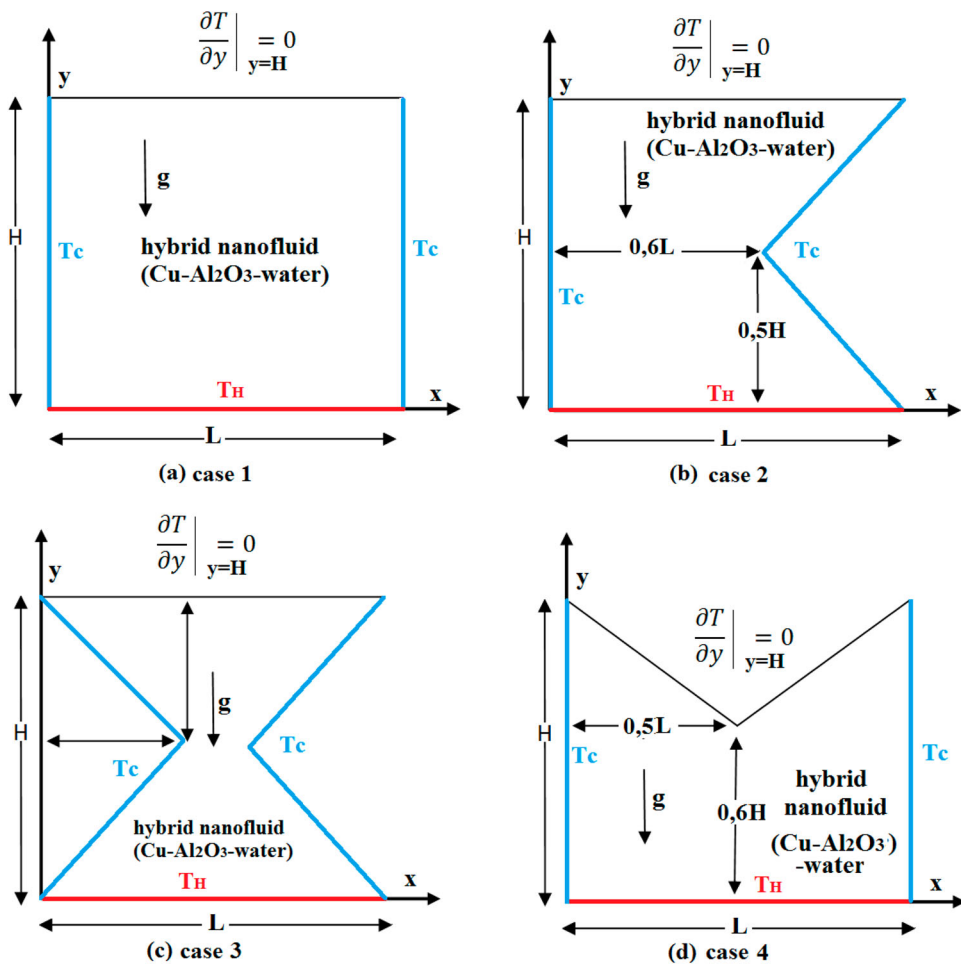


Figure 1. Schematization of the four cases of cavities ( $L = H$ ).

- The radiation heat transfers negligible

\*The thermo-physical properties of the hybrid nanofluid inside the cavity are constant except for the density for which the variations due to the temperature differences generate the movement, i. e. the Boussinesq hypothesis is considered to be applicable.

#### 4. Mathematical formulation

The equations governing the problem are:

- The continuity equation is written as follows:

$$\frac{\partial u}{\partial x} + \frac{\partial v}{\partial y} = 0 \tag{6}$$

- The momentum equations along the x-axis and the y-axis are expressed by:

$$u \frac{\partial u}{\partial x} + v \frac{\partial u}{\partial y} = \frac{1}{\rho_{hnf}} \left[ -\frac{\partial p}{\partial x} + \mu_{hnf} \left( \frac{\partial^2 u}{\partial x^2} + \frac{\partial^2 u}{\partial y^2} \right) \right] \quad (7)$$

$$u \frac{\partial v}{\partial x} + v \frac{\partial v}{\partial y} = \frac{1}{\rho_{hnf}} \left[ -\frac{\partial p}{\partial y} + \mu_{hnf} \left( \frac{\partial^2 v}{\partial x^2} + \frac{\partial^2 v}{\partial y^2} \right) + (\rho\beta)_{hnf} g(T - T_c) \right] \quad (8)$$

- The energy equation is expressed by:

$$u \frac{\partial T}{\partial x} + v \frac{\partial T}{\partial y} = \alpha_{hnf} \left( \frac{\partial^2 T}{\partial x^2} + \frac{\partial^2 T}{\partial y^2} \right) \quad (9)$$

With  $\alpha_{hnf} = \frac{k_{hnf}}{(\rho C_p)_{hnf}}$

To reduce the previous equations to a dimensionless form, it is necessary to define the following changes of variables:

$$X = \frac{x}{L}; \quad Y = \frac{y}{L}; \quad D = \frac{\alpha_f}{L}; \quad U = \frac{u}{D}; \quad V = \frac{v}{D}; \quad \theta = \frac{T - T_c}{T_H - T_c}; \quad P = \frac{p}{D^2 \rho_{hnf}}$$

The system of equations in dimensionless form:

- The continuity equation :

$$\frac{\partial U}{\partial X} + \frac{\partial V}{\partial Y} = 0 \quad (10)$$

- The momentum equations:

$$U \frac{\partial U}{\partial X} + V \frac{\partial U}{\partial Y} = -\frac{\partial P}{\partial X} + \frac{\mu_{hnf}}{\rho_{hnf} \alpha_f} \left( \frac{\partial^2 U}{\partial X^2} + \frac{\partial^2 U}{\partial Y^2} \right) \quad (11)$$

$$U \frac{\partial V}{\partial X} + V \frac{\partial V}{\partial Y} = -\frac{\partial P}{\partial Y} + \frac{\mu_{hnf}}{\rho_{hnf} \alpha_f} \left( \frac{\partial^2 V}{\partial X^2} + \frac{\partial^2 V}{\partial Y^2} \right) + (\rho\beta)_{hnf} \frac{1}{\rho_{hnf} \beta_f} Ra Pr \theta \quad (12)$$

- The energy equation :

$$U \frac{\partial \theta}{\partial X} + V \frac{\partial \theta}{\partial Y} = \frac{\alpha_{hnf}}{\alpha_f} \left( \frac{\partial^2 \theta}{\partial X^2} + \frac{\partial^2 \theta}{\partial Y^2} \right) \quad (13)$$

The Rayleigh number is defined as follows:

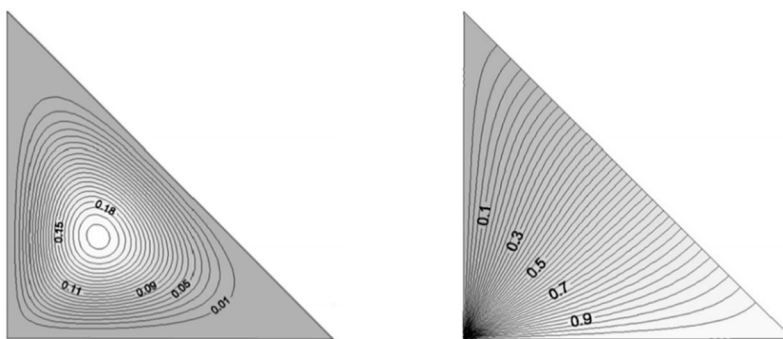
$$Ra = Gr.Pr = \frac{(\beta)_{hnf} g (T_H - T_c) L^3}{\nu_{hnf}^2} \times \frac{\nu_{hnf}}{\alpha_{hnf}} = \frac{(\beta)_{hnf} g (T_H - T_c) L^3}{\nu_{hnf} \alpha_{hnf}}$$

The local Nusselt number calculated at the cavity's bottom wall is expressed by [20]

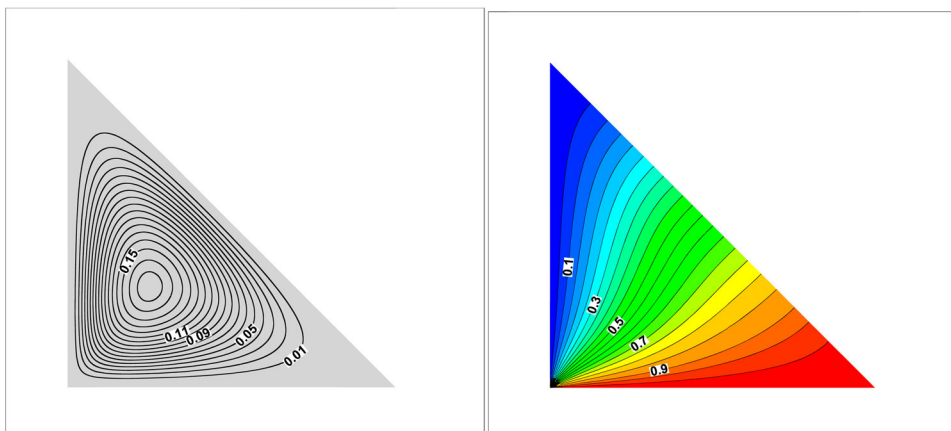
$$Nu_L = -\frac{k_{hnf}}{k_f} \left( \frac{\partial \theta}{\partial Y} \right)_{Y=0} \quad (14)$$

The average Nusselt number calculated at the cavity's bottom wall is expressed by [20]:

$$Nu_{ave} = \int_0^1 Nu_L dX \quad (15)$$



(a)



(b)

**Figure 2.** Streamlines (left) and isotherms (right) for  $Ra = 10^3$  (a) the numerical results [21] (b) This study results.

## 5. Validation and comparison of the results

Figure 2 shows a comparison between the streamlines and the isotherms plotted in this study for  $Ra = 10^3$  in the right-angled triangular cavity and those found by Yesiloz et al. [21]. On the other hand, Figure 3 represents another comparison between our isotherms for  $Ra = 5 \times 10^6$  with  $\Delta T = 11.6K$  in a quadrantal cavity at an inclination angle equal to 0 and those plotted in the work of Gurkan et al. [22]. From Figures 2 and 3, it can be concluded that there is a good agreement between the results of this work and those obtained in the two works [21] and [22], which confirms the validity of our numerical results.

## 6. Grid independence examination

In this work, a quadrilateral mesh is chosen in the two directions  $(x, y)$ ; after the simulation calculations converged, we tested the mesh independently. From Figure 4, which shows the dimensionless temperature variation along the plane  $y = 0.25H$  for the different cells

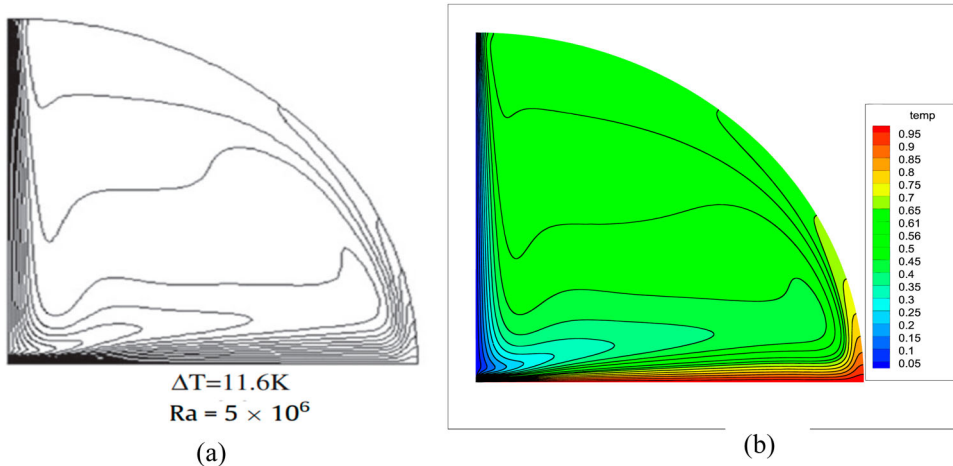


**Figure 3.** Numerical isotherms in a quadrantal cavity at an angle of inclination equal to 0 (a) Numerical results [22], (b) This study results.

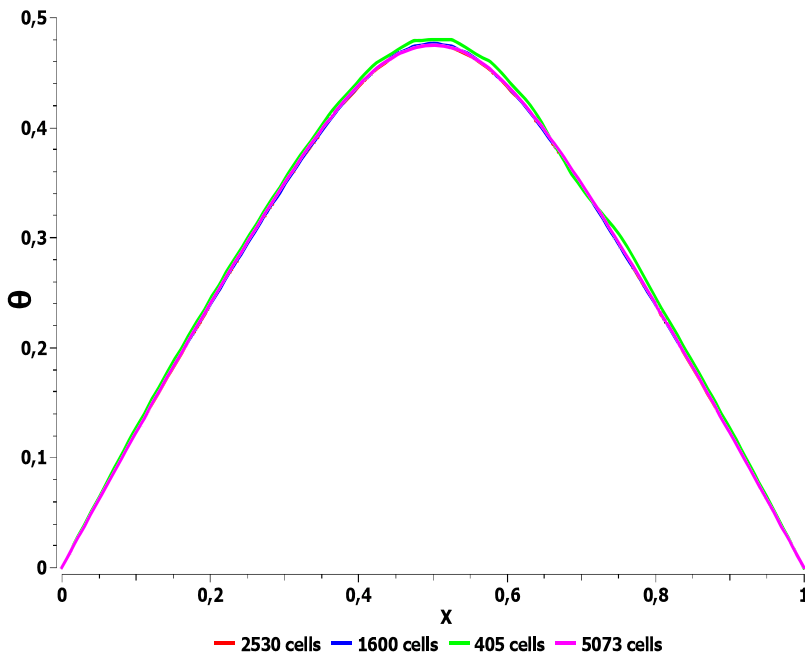
applied to the cavity in the first case, it can be seen that the temperatures are nearly identical. On the other hand, Figure 5 shows the influence of the number of nodes on the solution expressed by the profile of the average Nusselt number ( $Nu_{ave}$ ) of the bottom wall of the cavity in the first case in terms of the number of nodes according to the results of Figure 5. We conclude that when the number of nodes is 5000 nodes and more, the value of the average  $Nu$  number is independent of the mesh.

## 7. Results and discussions

In this paragraph, all the results obtained in this study by the fluent software in the form of current lines, isothermal and variations of the Nusselt number for the four cases studied will be highlighted.

Figure 6 a,b and c show the isotherms for the four cases and different values of the  $Ra$ . The temperature profiles show tight lines around the heat source, i. e.; the temperature gradient becomes higher near this heated wall which implies an increase in heat transfer through the bottom wall of the enclosure. These isotherms have a symmetrical shape in the first, the third and the fourth case at each  $Ra$ . Furthermore, the shape of the cavity has a considerable effect on the isotherms, and this becomes clearer at significant values of the  $Ra$  number, according to the results shown in Figure 6 a,b and c. The contours of the isotherms in the third case are close to the heat source for  $Ra = 10^5$ . This indicates that there is good heat exchange between the hybrid nanofluid and the hot bottom wall of the cavity, which improves the heat exchange rate.

Figure 7 a,b and c show streamlines for the four cases and different values of the  $Ra$ . It is noticeable that the value of  $Ra = 10^3$  (Figure 7a), the values of the streamlines are almost zero, in the order of  $10^{-5}$  and  $10^{-6}$  for the four cases. On the other hand, when the  $Ra$  number is increased and for  $Ra = 10^5$  (Figure 7c), the values of the streamlines are in the order of  $10^{-3}$  and  $10^{-4}$ . We also find that the shape of the enclosure has a significant effect on the stream-lines structures.



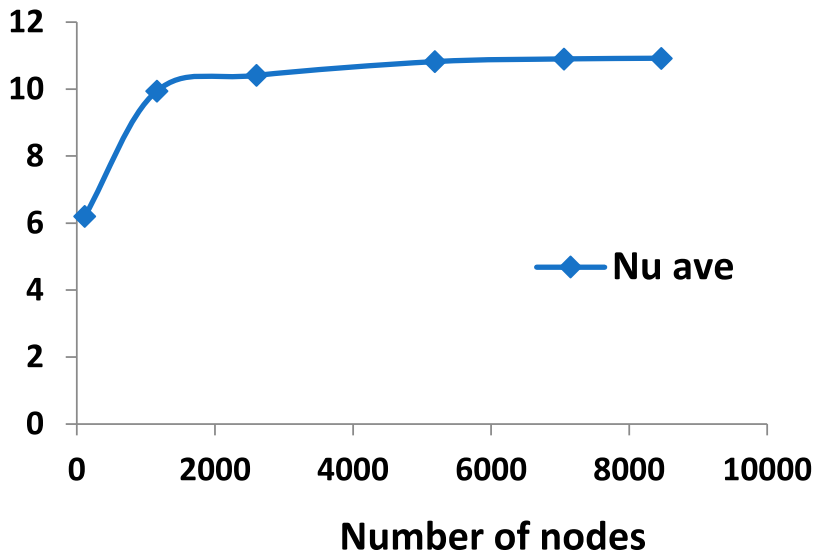
**Figure 4.** Influence of the mesh on the dimensionless temperature along the plane  $y = 0.25H$  of the cavity for case 1 and  $Ra = 10^4$ .

Figure 8 a and b show the dimensionless temperature evolution along two planes  $y = H/2$  and  $y = H/4$ , for the four cases studied and for Cu-Al<sub>2</sub>O<sub>3</sub>/water hybrid nanofluid. Figure 8a, show that the dimensionless temperature decreases near the sides of the cavity in all cases and rises in the middle of the cavity at  $x = L/2$  in the first, the third and the fourth case. In the second case, the temperature's peak is recorded at  $x = 0.2L$ , which is due to the asymmetrical shape of the cavity. We also note that the dimensionless temperature values in the third cavity case are low compared to the other cases, and this is due to the small length of the cavity at  $x = [0.4L - 0.6L]$  and  $y = H/2$ , where the fluid flow velocity is high. Other wise, we see at the  $y = H/4$  a plane where the dimensionless temperature values in all cases are high in the middle of the cavity at  $x = L/2$  as shown in Figure 8b.

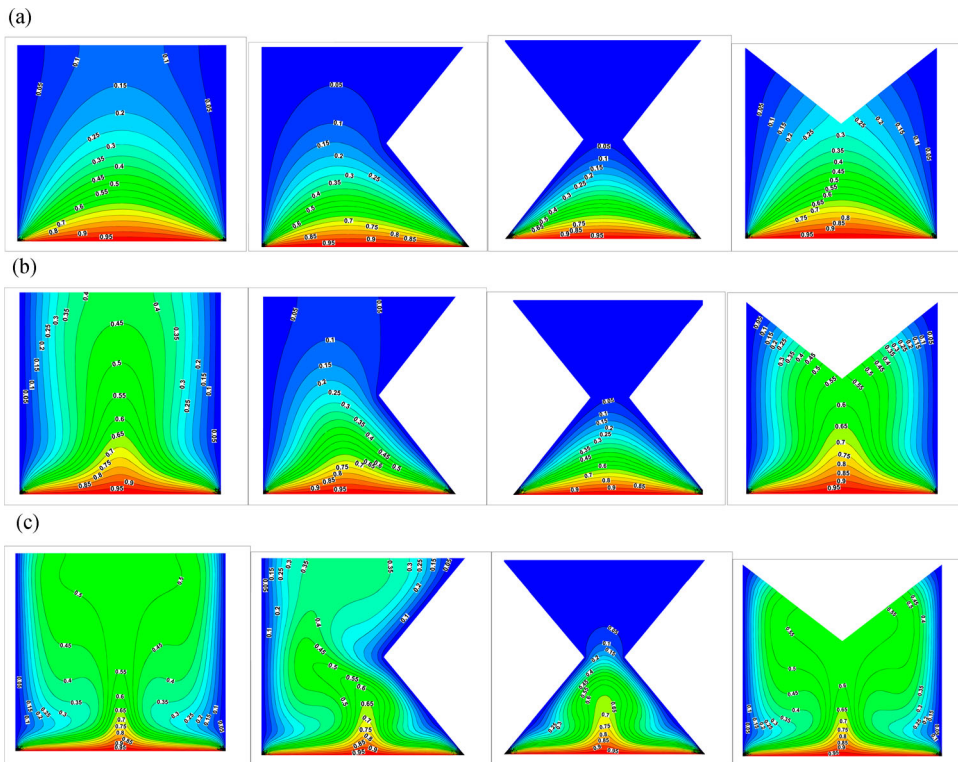
From a physical point of view, this presented study reveals that the phenomenon of heat transfer is related to both Rayleigh number, cavity shape and the movement velocity of nanoparticles in the base liquid.

Thus, the increase in the Rayleigh number leads to an increase in heat transfer and, therefore, a faster liquid flow. The flow speed helps the nanoparticles to move quickly inside the base liquid and makes the heat transfer process between the particles suitable, and the cavity's shape helps the heat exchange process.

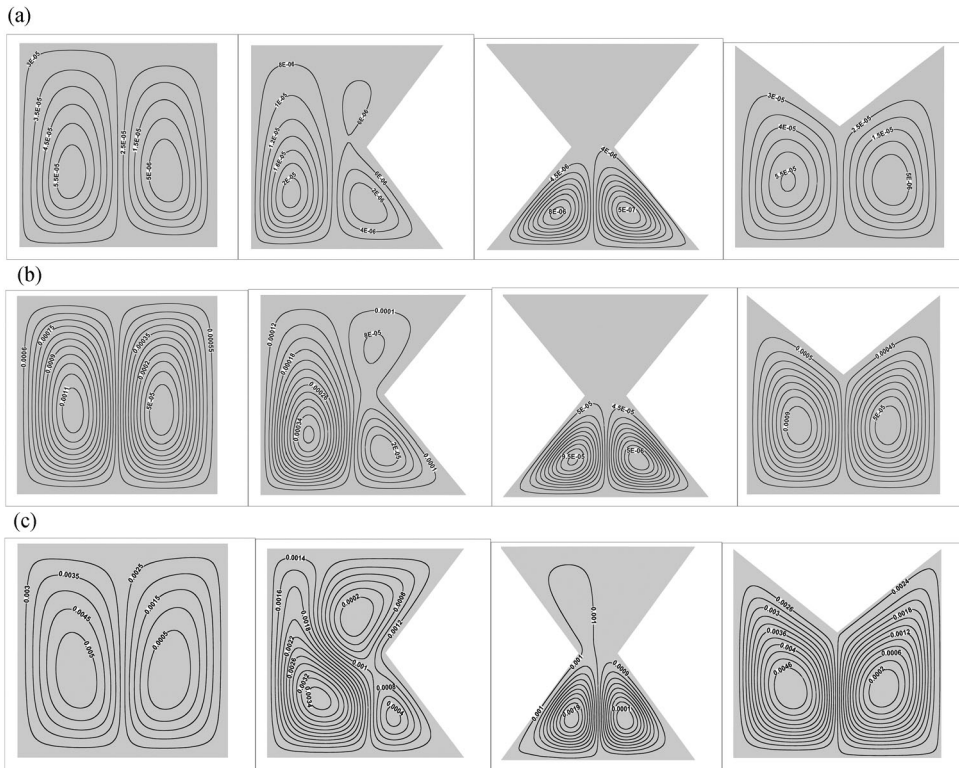
The cavity shape in the third case is characterized by its ability to improve heat exchange by changing the shape of the side walls of the cavity and making it convergent-divergent nozzle geometry to increase the fluid velocity at the coordinates  $(x = 0.5L, y = 0.5H)$  and this is with the help of gravity, on the other hand, we found that when changing the shape of one side wall (case 2- case 4) does not meet the desired purpose. The fluid velocity remains insufficient to improve the heat exchange inside the cavity.



**Figure 5.** Influence of the mesh on the average  $Nu$  number of the bottom wall of the cavity for case 1 and  $Ra = 10^5$ .



**Figure 6.** a. Isotherms for the four cases and for  $Ra = 10^3$  ( $\varphi = 0.03$ ). b. Isotherms for the four cases and for  $Ra = 10^4$  ( $\varphi = 0.03$ ). c. Isotherms for the four cases and for  $Ra = 10^5$  ( $\varphi = 0.03$ ).

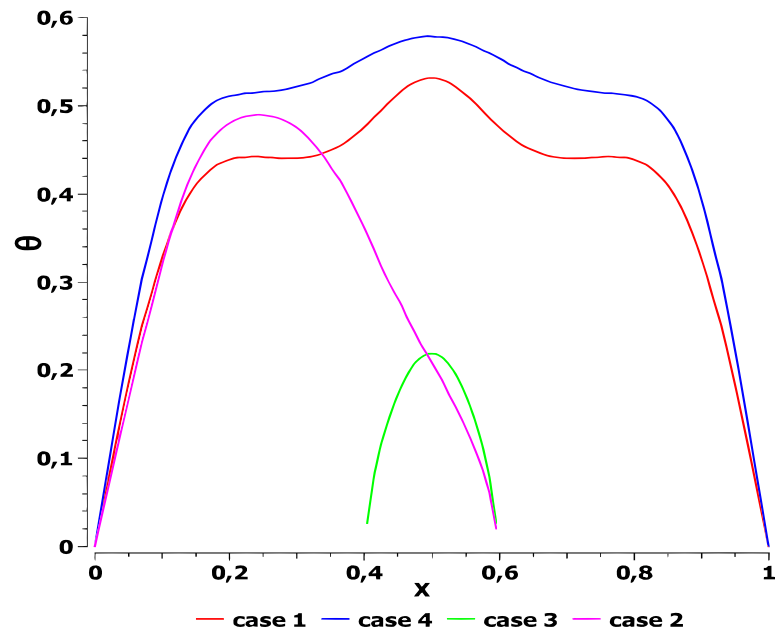
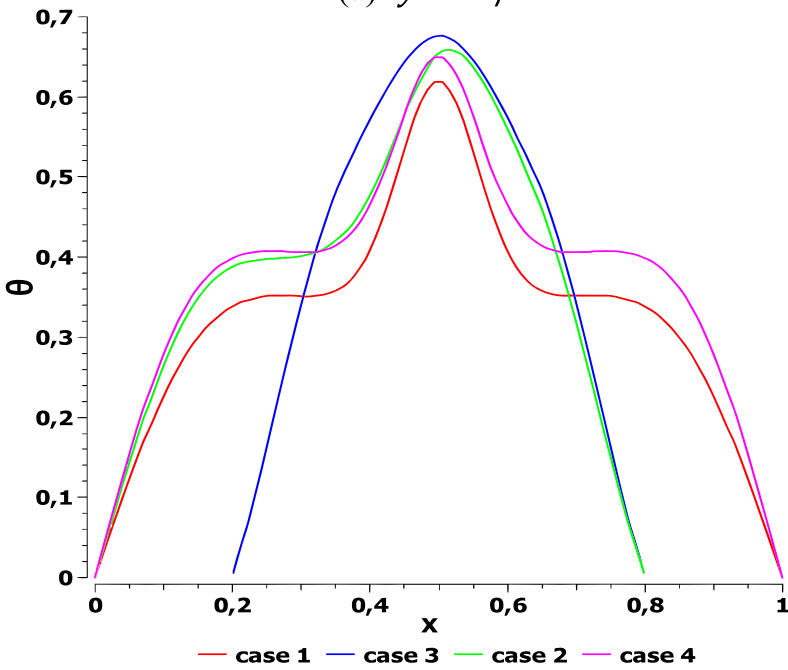


**Figure 7.** a. Streamlines for the four cases and for  $Ra = 10^3$  ( $\varphi = 0.03$ ). b. Streamlines for the four cases and for  $Ra = 10^4$  ( $\varphi = 0.03$ ). c. Streamlines for the four cases and for  $Ra = 10^5$  ( $\varphi = 0.03$ ).

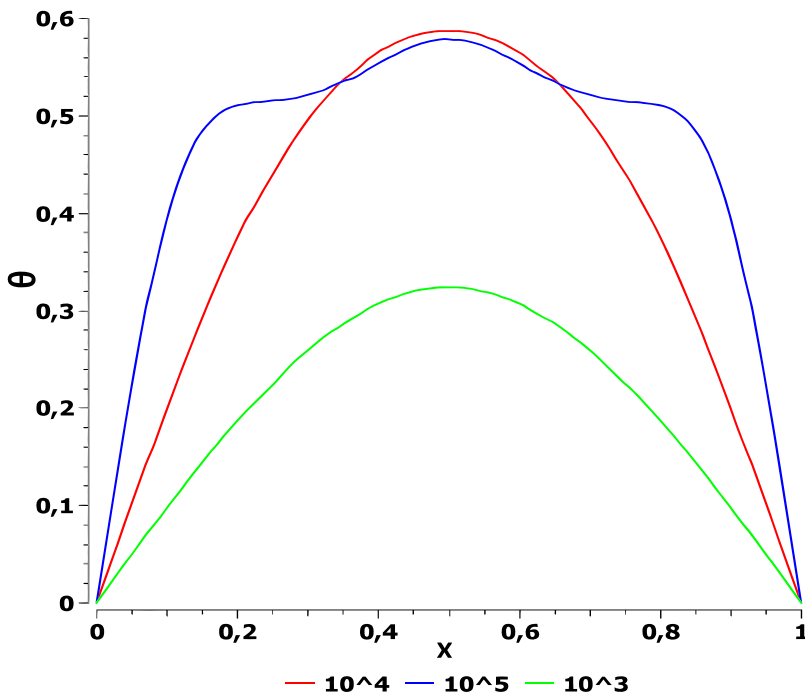
Figure 9 shows the dimensionless temperature evolution along the plane  $y = H/2$  in the fourth case of the cavity for different values of  $Ra$ . According to this study's results, we note that when  $Ra$  increases, the dimensionless temperature in the plane  $y = H/2$  increases as the temperature transition within the hybrid nanofluid increases with increasing flow velocity and the increasing movement of the  $\text{Cu-Al}_2\text{O}_3$  nanoparticles in the base fluid (water).

Figure 10 presents the evolution of the local  $Nu$  along the lower wall (hot wall) for different values of  $Ra$ . This figure shows that  $Nu$  decreases as we move along the lower wall to its middle, which is for all the values of  $Ra$ . This is because the hybrid nanofluid, which is at a low temperature compared to the wall, comes into contact with the hot wall and thus receives a quantity of heat (due to the large temperature gradient).

The evolution of the  $Nu_{ave}$  as a function of  $Ra$  for the four cases (arranged from left to right) and the hybrid nanofluid with a nanoparticle volume fraction equal to 0.03 is presented in Figure 11. It is noticeable that in the four cavity cases, the  $Nu_{ave}$  increases with  $Ra$ , but the  $Nu_{ave}$  values for the third cavity case are higher than in the three cases. This is due to the shape of the cavity and its effectiveness in increasing heat transfer.

(a)  $y = H/2$ (b)  $y = H/4$ 

**Figure 8.** The dimensionless temperature evolution along the plane (a)  $y = H/2$  and (b)  $y = H/4$  for the four cases studied and for hybrid nanofluid ( $\varphi = 0.03$ ).



$$y = H/2$$

**Figure 9.** Evolution of the dimensionless temperature along the plane  $y = H/2$  in case 4.

## 8. Conclusion

This study presents a numerical investigation of the laminar regime and the impact of the geometric form of the cavity by using Cu-Al<sub>2</sub>O<sub>3</sub>-water hybrid nanofluid with a solid volume fraction equal to 0.03 and using the commercial software, ANSYS Fluent 17.0.

The acquired results are represented in the form of profiles of streamlines, isotherms, and Nusselt number for the different shapes of the cavity as a function of the Rayleigh number (between 10<sup>3</sup> and 10<sup>5</sup>); the results obtained led to the following observations:

- For low values of the Rayleigh number (10<sup>3</sup>, 10<sup>4</sup>) The heat transfer takes place mainly by conduction in the cavity.
- The shape of the cavity in the third case gives the best heat exchange compared to the other cases, and the increase in the value of the Rayleigh number contributes to an enhancement in heat exchange, especially in the third case. It also participates in a decrease in the temperature inside the cavity.
- According to the simulation results and for the remaining three forms, the cavity shape in the second case gives better heat exchange than in the fourth and first cases.

These results will be used for the design and the improvements of the cavity.

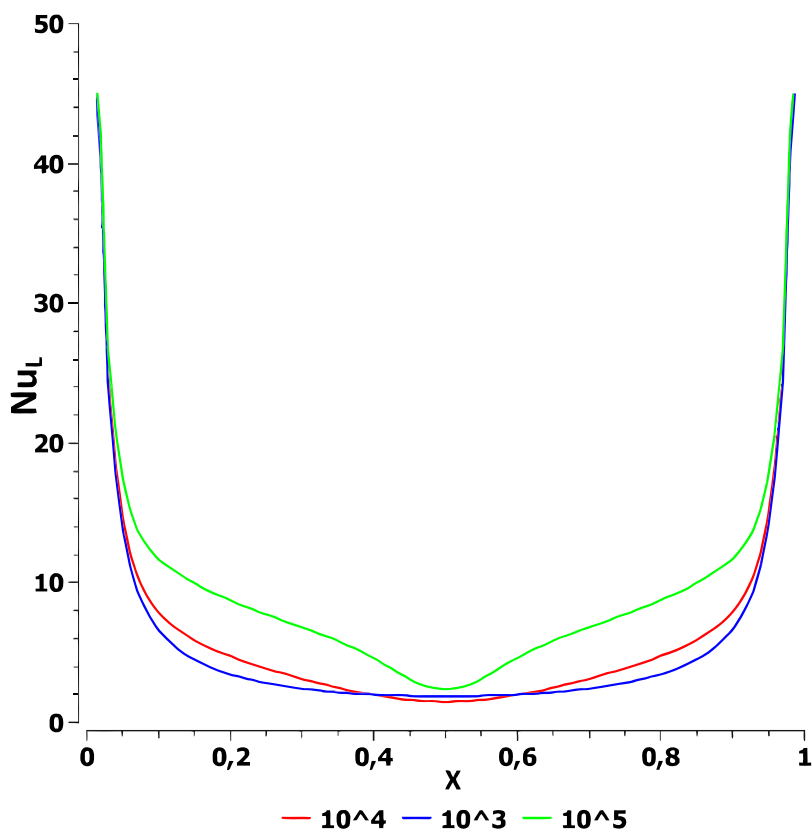


Figure 10. Local  $Nu$  profile along the hot bottom wall for different  $Ra$  values.

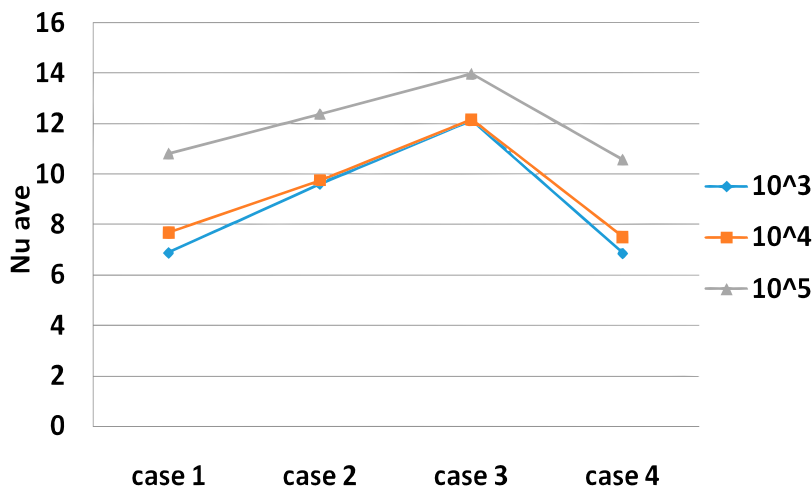


Figure 11. Average  $Nu$  variation with  $Ra$  for the four cases studied.

## Disclosure statement

No potential conflict of interest was reported by the author(s).

## References

- [1] Mahmoodi M, Sebdani SM. Natural convection in a square cavity containing a nanofluid and an adiabatic square block at the center. *Superlattices Microstruct.* 2012;52:261–275.
- [2] Aminossadati SM. Hydromagnetic natural cooling of a triangular heat source in a triangular cavity with water-CuO nanofluid. *Int Commun Heat Mass Transfer.* 2013;43:22–29.
- [3] Mehmood K, Hussain S, Sagheer M. Numerical simulation of MHD mixed convection in alumina-water nanofluid filled square porous cavity using KKL model: effects of non-linear thermal radiation and inclined magnetic field. *J Mol Liq.* 2017;238:485–498.
- [4] Rahmati AR, Tahery AA. Numerical study of nanofluid natural convection in a square cavity with a hot obstacle using lattice Boltzmann method. *Alexandria Eng J.* 2018;57:1271–1286.
- [5] Ma Y, Mohebbi R, Rashidi MM, et al. MHD convective heat transfer of Ag-MgO/water hybrid nanofluid in a channel with active heaters and coolers. *Int J Heat Mass Transf.* 2019;137:714–726.
- [6] Ghalambaz M, Doostani A, Izadpanahi E, et al. Conjugate natural convection flow of Ag-MgO/water hybrid nanofluid in a square cavity. *J Therm Anal Calorim.* 2020;139:2321–2336.
- [7] Rizwan UH, Aman S. Water functionalized CuO nanoparticles filled in a partially heated trapezoidal cavity with inner heated obstacle: FEM approach. *Int J Heat Mass Transf.* 2019;128:401–417.
- [8] Chakkingal M, Schiavo S, Ataei-Dadavia I, et al. Effect of packing height and location of porous media on heat transfer in a cubical cavity: are extended Darcy simulations sufficient? *Int J Heat Fluid Flow.* 2020;84:108617.
- [9] Armaghani T, Sadeghi MS, Rashad AM, et al. MHD mixed convection of localized heat source/sink in an  $Al_2O_3$ -Cu/water hybrid nanofluid in L-shaped cavity. *Alexandria Eng J.* 2021;60:2947–2962.
- [10] Khan NH, Paswan MK, Hassan MA. Natural convection of hybrid nanofluid heat transport and entropy generation in cavity by using Lattice Boltzmann method. *J Indian Chem Soc.* 2022;99(3):100344.
- [11] Alsabery AI, Tayebi T, Kadhimi HT, et al. Impact of two-phase hybrid nanofluid approach on mixed convection inside wavy lid-driven cavity having localized solid block. *J Adv Res.* 2021;30:63–74.
- [12] Geridonmez BP, Oztop HF. Natural convection of hybrid nanofluid flow in the presence of multiple vertical partial magnetic fields in a trapezoidal shaped cavity. *The European Physical Journal Special Topics.* 2022;231:2761–2771.
- [13] Raizah Z, Aly AM, Alsedais N, et al. MHD mixed convection of hybrid nanofluid in a wavy porous cavity employing local thermal non-equilibrium condition. *Sci Rep.* 2021;11(1):1–22.
- [14] Sudarsana Reddy P, Sreedevi P. Effect of thermal radiation on heat transfer and entropy generation analysis of MHD hybrid nanofluid inside a square cavity. *Waves Random Complex Media.* 2022. <https://www.tandfonline.com/doi/full/10.1080/17455030.2021.2023780>
- [15] Gürdal M, Pazarlıoğlu HK, Tekir M, et al. Implementation of hybrid nanofluid flowing in dimpled tube subjected to magnetic field. *Int Commun Heat Mass Transfer.* 2022;134:106032.
- [16] Haokun Z, Yit Fatt Y. Modeling of hybrid nanofluid flow and heat transfer in a porous curved channel. *AIP Conf Proc.* 2022;2425:020003.
- [17] Zainal NA, Nazar R, Naganthran K, et al. Slip effects on unsteady mixed convection of hybrid nanofluid flow near the stagnation point. *Appl Math Mech.* 2022;43:547–556.
- [18] Gorla RSR, Siddiqa S, Mansour MA, et al. Heat source/sink effects on a hybrid nanofluid-filled porous cavity. *J Thermophys Heat Transfer.* 2017;31(4).
- [19] Aminossadati SM, Ghasemi B. Natural convection cooling of a localised heat source at the bottom of a nanofluid-filled enclosure. *Eur J Mech B Fluids.* 2009;28(5):630–640.
- [20] Alsabery AI, Ishak MS, Chamkha AJ, et al. Entropy generation analysis and natural convection in a nanofluid-filled square cavity with a concentric solid insert and different temperature distributions. *Entropy.* 2018;20:336, doi:10.3390/e20050336.

- [21] Yesiloz G, Aydin O. Laminar natural convection in right-angled triangular enclosures heated and cooled on adjacent walls. *Int J Heat Mass Transf.* 2013;60:365–374.
- [22] Yesiloz G, Aydin O. Natural convection in an inclined quadrantal cavity heated and cooled on adjacent walls. *Exp Therm Fluid Sci.* 2011;35:1169–1176.